Since January 2020 Elsevier has created a COVID-19 resource centre with free information in English and Mandarin on the novel coronavirus COVID-19. The COVID-19 resource centre is hosted on Elsevier Connect, the company's public news and information website.

European Journal of Pharmaceutical Sciences 151 (2020) 105386

Contents lists available at ScienceDirect

European Journal of Pharmaceutical Sciences

journal homepage: www.elsevier.com/locate/ejps

Discovery of 2-aryl and 2-pyridinylbenzothiazoles endowed with antimicrobial and aryl hydrocarbon receptor agonistic activities

Elizabeth Goya-Jorge[a,b,1], Fatma Abdmouleh[c,d,1], Laureano E. Carpio[b], Rosa M. Giner[a], Maité Sylla-Iyarreta Veitía[c,*]

[a] Departament de Farmacologia, Facultat de Farmàcia, Universitat de València. Av. Vicente Andrés Estellés, s/n, 46100 Burjassot, Valencia, Spain
[b] ProtoQSAR SL. CEEI (Centro Europeo de Empresas Innovadoras), Parque Tecnológico de Valencia, Av. Benjamin Franklin 12, 46980 Paterna, Valencia, Spain
[c] Equipe de Chimie Moléculaire du Laboratoire Génomique, Bioinformatique et Chimie Moléculaire (EA 7528), Conservatoire National des Arts et Métiers (Cnam), 2 rue Conté, 75003, HESAM Université, Paris, France.
[d] Laboratoire de Biotechnologie Microbienne et d'Ingénierie des Enzymes (LBMIE). Centre de Biotechnologie de Sfax, Université de Sfax, Route de Sidi Mansour Km 6, BP 1177, 3018, Sfax, Tunisie.

ARTICLE INFO

Keywords:
Benzothiazole
Antibacterial
Antifungal
Antibiofilm
Ah receptor
Agonism

ABSTRACT

Benzothiazole is a privileged scaffold in medicinal chemistry present in diverse bioactive compounds with multiple pharmacological applications such as analgesic, anticonvulsant, antidiabetic, anti-inflammatory, anticancer and radioactive amyloidal imagining agents. We reported in this work the study of sixteen functionalized 2-aryl and 2-pyridinylbenzothiazoles as antimicrobial agents and as aryl hydrocarbon receptor (AhR) modulators. The antimicrobial activity against Gram-positive (*S. aureus* and *M. luteus*) and Gram-negative (*P. aeruginosa, S. enterica* and *E. coli*) pathogens yielded MIC ranging from 3.13 to 50 μg/mL and against the yeast *C. albicans*, the benzothiazoles displayed MIC from 12.5 to 100 μg/mL. All compounds showed promising antibiofilm activity against *S. aureus* and *P. aeruginosa*. The arylbenzothiazole **12** displayed the greatest biofilm eradication in *S. aureus* (74%) subsequently verified by fluorescence microscopy. The ability of benzothiazoles to modulate AhR expression was evaluated in a cell-based reporter gene assay. Six benzothiazoles (**7, 8-10, 12, 13**) induced a significant AhR-mediated transcription and interestingly compound **12** was also the strongest AhR-agonist identified. Structure-activity relationships are suggested herein for the AhR-agonism and antibiofilm activities. Furthermore, *in silico* predictions revealed a good ADMET profile and druglikeness for the arylbenzothiazole **12** as well as binding similarities to AhR compared with the endogenous agonist FICZ.

1. Introduction

The interaction with microorganisms is fundamental to produce nutrients and to suppress the pathogen colonization in the mucous membranes of healthy hosts. Microbial communities are playing important roles in organ development, metabolism, and immune homeostasis (Sommer and Bäckhed, 2013). However, the diseases triggered by infectious agents have caused most of the biggest health tragedies of mankind. The coronavirus SARS-CoV-2 responsible for the COVID-19 pandemic is a current example (Shereen et al., 2020). The preservation of health against pathogenic colonization is determined by the immune response as well as the adequate biotransformation of toxicants in the host cells (Janeway et al., 2001). The transformation and appearance of new pathogens and the so-called emerging diseases, as well as the adaptive resistance to pharmacological treatments, mean that all efforts are insufficient for the control and/or eradication of infections.

The aryl hydrocarbon receptor (AhR) is a long known chemical sensor highly expressed in the liver and in barrier organs (Esser and Rannug, 2015). Despite the extensive association of AhR activation with dioxin-like toxicity during several decades, nowadays is well known that agonist modulations upon AhR can lead to physiotherapeutical benefits in multiple pathological conditions (Hu et al., 2007; Zhao et al., 2019). AhR activity regulates, among others, the immune system functions, through direct or indirect paths, and the differentiation of diverse immune cell types (Esser et al., 2009). Important roles of AhR are suggested in infective disease tolerance and in defense pathways. As an example, the influence of AhR in primary LPS

* Corresponding author.
E-mail address: maite.sylla@lecnam.net (M. Sylla-Iyarreta Veitía).
[1] authors contributed equally to this work

https://doi.org/10.1016/j.ejps.2020.105386
Received 16 April 2020; Received in revised form 15 May 2020; Accepted 19 May 2020
Available online 27 May 2020

ADMET	absorption, distribution, metabolism, and excretion - toxicity	FA	fusidic acid
AhR	aryl hydrocarbon receptor	FICZ	5,11-dihydroindolo[3,2-b]carbazole-12-carbaldehyde
AhR-HepG2, Lucia™	human hepatoma cell line stably transfected to express AhR	Lv	levofloxacin
BT	benzothiazole	MBC	Minimal Bactericidal Concentration
CH223191	2-methyl-2H-pyrazole-3-carboxylic acid	MIC	Minimal Inhibitory Concentration
CYP	cytochrome P450	MTT	3-(4,5-dimethyl thiazol-2-yl)-2,5-diphenyl tetrazolium bromide
Eff	efficiency	OD	optical density

responsiveness and in fact the induction of endotoxin tolerance has been demonstrated using a *Streptococcus*-induced multifocal septic arthritis model. The endotoxin-tolerant state LPS triggered was found to protect mice against immunopathology in Gram-positive infections, steering the contribution of AhR to host fitness (Bessede et al., 2014) . Moreover, AhR plays a key role in innate defense against bacteria. Bacterial pigmented virulence factors such as the phenazines from *P. aeruginosa* and the naphthoquinone phthiocol from *M. tuberculosis*, have been characterized, as ligands of AhR. During ligand binding, AhR activation leads to degradation of virulence factor and regulation of cytokine and chemokine production. Therefore, AhR recognition of these bacterial pigments is reported as a prominent alternative path to control the antibacterial response. It has also been shown that AhR activation regulates inflammatory leukocyte recruitment to the infected lung and control of bacterial replication demonstrating that AhR plays a central role in defense against both acute and chronic bacterial infection (Moura-Alves et al., 2014). Besides its protective effect against intestinal pathogenic bacteria, AhR is also involved in resistance to fungi. It has been described that some indole-type AhR ligands dramatically inhibit *Candida albicans* biofilm formation, as well as attachment to intestinal epithelial cells suggesting that AhR activation may be a potential therapeutic target to combat bacterial and fungal intestinal infection (Oh et al., 2012).

Benzothiazole (BT) is a heterocyclic structure bearing a benzene ring fused with a five-membered ring containing nitrogen and sulfur atoms. The BT nucleus is considered a privileged structure particularly important in medicinal chemistry due to the wide range of pharmacological applications ascribed to its derivatives (Ali and Siddiqui, 2013; Bondock et al., 2010; Choudhary et al., 2017; Gill et al., 2015). Anticancer, antimicrobial, and anti-inflammatory are among the most extensively reported clinical uses of this versatile fused heterocyclic scaffold (Kamal et al., 2015). Furthermore, BT skeleton is present in imaging agents and as radiotracers of positron emission tomography (PET) used to diagnose neurological diseases and in biocidal agents employed as industrial chemicals (Mathis et al., 2003; Muthusubramanian et al., 2001). Some examples of widely used benzothiazoles are represented in Figure 1.

In 2013, encouraged by the high interest in [^{11}C] PIB for diagnosing Alzheimer's disease, we developed a new series of 2-arylbenzothiazoles and 2-pyridinylbenzothiazole derivatives by Szuki-Miyaura coupling reaction. The one-step protocol was performed from commercially available reactants to obtain the desired radiopharmaceutical precursors in high yields under thermal conditions or microwave activation, Scheme 1 (Bort et al., 2013).

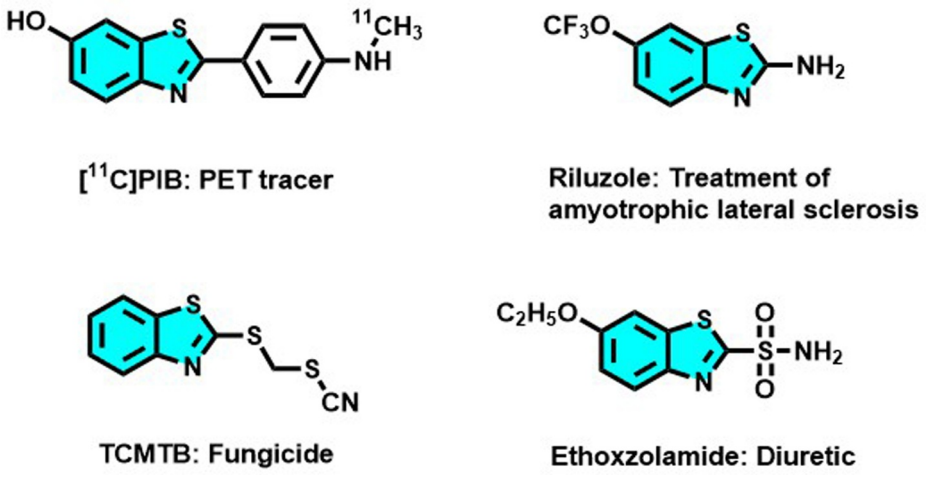

Figure 1. Examples of marketed benzothiazoles and their main applications (Hergesheimer et al., 2015; Mathis et al., 2003; Moyer and Ford, 1958; Muthusubramanian et al., 2001)

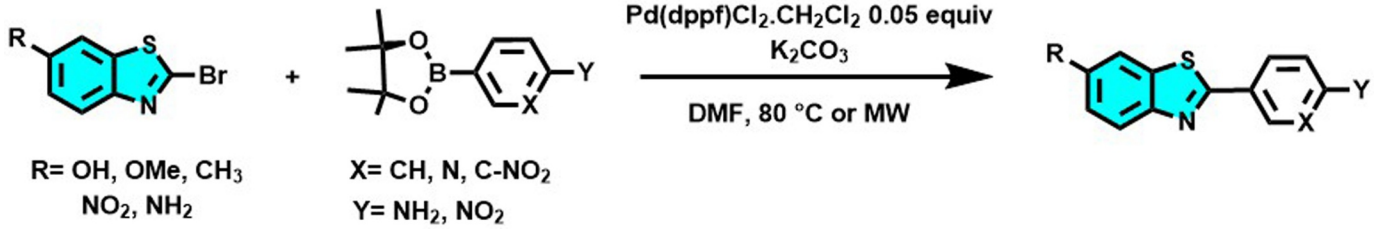

Scheme 1. Synthesis of a new series of arylbenzothiazoles, potential precursors of the radiochemical tracer [^{11}C]PIB, by Suzuki-Miyaura coupling reaction (Bort et al., 2013).

Inspired by the therapeutic potentialities of the benzothiazole scaffold and taking into account the aforementioned pharmacological interest of combining antimicrobial and AhR-modulatory activities we investigate the antimicrobial potential of a series of sixteen arylbenzothiazoles, previously synthesized in our laboratory, against Gram positive and Gram negative pathogens and the opportunist yeast *C. albicans*. The AhR agonist/antagonist behavior of benzothiazoles was studied using an AhR reporter assay preceded by a viability study. The structure-activity relationships considerations between biocidal and AhR modulatory activities were also discussed herein.

2. Experimental Section

The thirteen 2-arylbenzothiazoles and the three 2-pyridinylbenzothiazoles biologically evaluated in this work were previously prepared by our team from the corresponding 2-bromobenzothiazoles (1 eq.) and phenylboronic acid pinacol ester (1.2 eq.) in anhydrous DMF, and in presence of K_2CO_3 (6.0 eq.) and Pd(dppf)Cl_2.CH_2Cl_2 (0.05 eq.). The reactions were performed under argon bubbling at 80 °C or under microwave irradiation and monitoring by TLC or by GC-MS. After treatment, the compounds were isolated by filtration as colored powders and the structures were checked by comparison of their NMR, IR, and HRMS data. The detailed synthetic procedures and characterization can be found in the original research article (Bort et al., 2013).

2.1. Biological studies

2.1.1. Antibacterial and antifungal activities

The *in vitro* antibacterial and antifungal activities of the studied benzothiazoles (**1**-**16**) were evaluated by using a microplate broth dilution assay according to the National Committee for Clinical Laboratory Standard (NCCLS. 2002). They were screened against the two Gram-positive pathogens *Staphylococcus aureus* (ATCC 9144) and *Micrococcus luteus* (LB14110) and the three Gram-negative *Salmonella enterica* (NCTC 6017), *Pseudomonas aeruginosa* (ATCC 9027), and *Escherichia coli* (ATCC 8739), and the yeast *Candida albicans* (ATCC 2091) by using microplate broth dilution assay according to the National Committee for Clinical Laboratory Standard (NCCLS. 2002). Serial dilutions of compounds, dissolved in DMSO, were prepared in LB broth medium (1% Bactotryptone, 0.5% Yeast extract, 0.5% NaCl).

A volume of 100 µL of the tested compounds (final concentration ranging from 200-1.15 µg/mL) and 100 µL of bacterial suspension (10^7 CFU/mL) was dispensed into each well of 96-well plates (Corning) and incubated at 37 C for 20 h. Levofloxacin and fusidic acid were used as positive controls. After the incubation period, the Minimal Inhibitory Concentrations (MICs) were recorded as the lowest concentrations of the compounds at which no visible growth occurred. The 3-(4,5-dimethyl thiazol-2-yl)-2,5-diphenyl tetrazolium bromide (MTT) reagent was added to each well to evaluate the microbial growth, indicating live cells when a color transformation from yellow to dark blue was observed. The Minimal Bactericidal Concentrations (MBCs) were determined by sampling one loopful from each well and cultured on plate count agar at 30 C for 24 h. The lowest concentration of compounds that resulted in microbial death was reported as their MBCs.

The optical density (OD) was measured at 600 nm using a microplate reader (Varioskan, Thermofisher). The antimicrobial activity was expressed as the inhibition percentage when compared with microbial culture untreated.

2.1.2. Antibiofilm activity

Biofilm formation in *S. aureus* and *P. aeruginosa* was determined spectrophotometrically by using the crystal violet test in 96-well plates as previously described (Ricco et al., 2020). The tested compounds (**1**-**16**) were assayed at their MIC against *S. aureus* and *P. aeruginosa*, respectively, to determine the biofilm anti-adhesion activity. In addition, the biofilm eradication activity of benzothiazoles was evaluated at 200 µg/mL. A volume of 100 µL of each BT/well was delivered into the plates. Then, 100 µL/well of a fresh overnight cultured bacterial suspension diluted was added until obtaining a final OD of 0.1 at 600 nm. After 24 h incubation at 37 ºC, the wells were emptied, gently rinsed twice with PBS, and the plates dried at 60 ºC for 45 min. The biofilm was stained with 150 µL of crystal violet solution (0.2%) for 15 min at room temperature. After staining, plates were rinsed with water and 200 µL/well of glacial acetic acid were added to dissolve the crystals. After 1 h incubation at room temperature, the OD of the adherent biofilm was measured at 570 nm using a microplate reader (Varioskan, Thermofisher). The antibiofilm activity was expressed as the inhibition percentage when compared with the negative control.

The antibiofilm activity against *S. aureus* of compound 4-(6-methyl-1,3-benzothiazol-2-yl)-2-nitroaniline (**12**) was also determined by fluorescence microscopy images (OLYMPUS Fluorescent microscope BX50 equipped with a digital camera OLYMPUS DP70). The biofilms grown on glass pieces (Ø 10 mm) and placed in 24-well polystyrene plates were treated with **12** at 50 µg/mL (MIC value against *S. aureus*) for the anti-adhesion test and at 200 µg/mL for the eradication test. Non-treated wells containing the LB medium served as control. The bacterial inoculation was adjusted to an OD 600 nm of 0.1. Plates were incubated at 37 °C for 24 h. The wells were carefully emptied, the glass slides washed with PBS, and 500 µL/well of acridine orange (0.1% in PBS) were added. A 40× objective using U-MWB2 filter with excitation at 460–490 nm and emission at 520 nm was used for the visualization.

2.1.3. Cell viability evaluation

Cell Line characteristics and maintenance. AhR-HepG2 Lucia™ cell line engineered from the human HepG2 hepatoma cell line was obtained from InvivoGen stably transfected to express the endogenous Ah receptor and thereby screening potential AhR ligands. Lucia luciferase reporter gene is coupled with the human *Cyp1a1*, while the Lucia luciferase reporter protein is readily measurable in the cell culture supernatant. According to the provider's recommendations, AhR-HepG2 cells were maintained in Minimum Essential Medium containing non-essential amino acids (MEM-NEAA, Gibco ThermoFisher Scientific) supplemented with 10% (v/v) fetal bovine serum (FBS), penicillin (100 U/mL), streptomycin (100 µg/mL) in a humidified 5% CO_2 atmosphere at 37 °C. Normocin (0.1 mg/mL) and Zeocin (0.2 mg/mL) from Invivogen were added to the culture medium after the third passage.

Cell viability bioassay. The reduction caused by dehydrogenases and other reducing agents present in metabolically active cells was evaluated following the colorimetric MTT assay (Mosmann, 1983), with the aim of avoiding misinterpretations caused by cell damage in AhR activity tests.

Briefly, AhR-HepG2 cells were trypsinized, seeded on 96-well plates at a density of 2.0×10^5 cells/mL, and cultured overnight in MEM-NEAA. Next, cells were treated during 24 h with 10 µL/well of 5 µM and 10 µM concentrations of the sixteen benzothiazoles, or else with the positive control ligands which were 5,11-dihydroindolo[3,2-b]carbazole-12-carbaldehyde (FICZ) for agonism, and 2-methyl-2H-pyrazole-3-carboxylic acid (CH223191) for antagonism. A volume of 100 µL/well of MTT reagent (0.5 mg/mL) was added to the emptied plates containing the cells attached. Approximately 3 h of incubation at 37 °C allowed the transformation of the yellow MTT to the water-insoluble violet-blue formazan that was dissolved by adding 100 µL/well of DMSO. The OD was measured by reading the absorbance at 490 nm using a microplate reader (VICTORx3, PerkinElmer Inc., USA).

2.1.4. AhR reporter assays

AhR agonist and antagonist bioassay. To measure the effects on AhR transcriptional activity, AhR-HepG2 cells were trypsinized, passed through 18-gauge (18G) needles, and a suspension of 2.0×10^5 cells/mL was seeded into 96-wells microplates (200 µL/well) in a MEM-NEAA medium without Normocin nor Zeocin. After 24 h of incubation at 37

°C, cells were exposed to the tested compounds during another 24 h. The treatment of cells in agonistic mode was conducted by adding 10 µL/well of 5 µM and 10 µM of the benzothiazoles. In antagonistic mode 10 µL/well of the benzothiazoles (or CH223191) were added followed by 10 µL/well of the EC_{50} determined for the known AhR agonist FICZ used as positive control.

A volume of 20 µL/well of the supernatant of treated cells was transferred to white sterile and flat-bottom 96-wells microplates (Corning). After 50 µL/well of the QUANTI-Luc™ assay reagent (Invivogen) was added and the luminescence immediately measured in a microplate reader (VICTORx3, PerkinElmer Inc., USA). Results were expressed as fold response and as efficiency (Eff) percentage relative to the activity displayed by the positive control FICZ.

2.2. Computational studies

ADMET profile and druglikeness. Physicochemical, biopharmaceutical, and toxicological properties of **12** were predicted using the software ADMET Predictor™ v9.5 (Simulations Plus, Inc., Lancaster, CA, USA) (Ghosh et al., 2016).

Molecular docking simulations. Molecular docking analysis was performed with Autodock Vina (Trott and Olson, 2009) as implemented in YASARA (Krieger and Vriend, 2014). The crystallized protein structure was obtained from the Protein Data Bank (PDB ID 3F1O). Benzothiazole **12** and the known agonist FICZ were the ligands used. Simulations were performed for the entire target structure making stiff the protein and flexible the ligand compounds. The interactions of the best protein/ligand complexes were predicted using the Protein-Ligand Interaction Profiler web server (Salentin et al., 2015). Molecular graphics and analyses were performed with UCSF Chimera (Pettersen et al., 2004).

3. Results and Discussion

3.1. Biological Evaluation

3.1.1. Antimicrobial activity

A set of BTs was screened for antibacterial activity against Gram-positive (*M. luteus* and *S. aureus*) and Gram-negative (*E. coli, P. aeruginosa*, and *S. enterica*) pathogen strains and the yeast *C. albicans*. The Minimal Inhibitory Concentration (MIC) and the Minimal Bactericidal Concentration (MBC) for the 16 tested benzothiazoles and for levofloxacin (Lv) and fusidic acid (FA), used as positive controls, are reported in Table 1. As shown, levofloxacin had a notable potency against all the pathogens with MICs and MBCs lower than 1.52 µg/mL as expected from this broad-spectrum fluoroquinolone (Keam et al., 2005). Meanwhile, the MICs for fusidic acid ranging from 12.5-25 µg/mL and the MBCs were 100 µg/mL in Gram positive bacteria and higher in the other microorganisms studied.

The functionalized 2-aryl and 2-pyridinylbenzothiazoles assayed showed in general good antimicrobial potency. The MBC/MIC ratio (≥ 4) indicated predominant bacteriostatic effects. The antibacterial activity did not reveal important differences in the potency of the benzothiazoles against Gram-positive and Gram-negative bacteria, although Gram-positive strains seem to be more sensitive.

The inhibition potency against *M. luteus* was the most relevant.

Table 1
Minimal inhibitory concentration (MIC) and Minimal bactericidal concentration (MBC) values exhibited by the BTs and the positive controls levofloxacin and fusidic acid.

ID	R	X	Y	[c][a]	Gram (+) *M. luteus*	*S. aureus*	Gram (-) *E. coli*	*P. aeruginosa*	*S. enterica*	Yeast *C. albicans*
1	OH	CH	NH_2	MIC	[6.25-12.5]	[6.25-12.5]	[12.5-25]	[12.5-25]	[12.5-25]	[12.5-25]
				MBC	100	100	>100	>100	100	>100
2	OH	N	NH_2	MIC	[12.5-25]	[12.5-25]	[12.5-25]	[25-50]	[12.5-25]	[12.5-25]
				MBC	100	>100	>100	>100	>100	>100
3	OH	CH	NO_2	MIC	[12.5-25]	[12.5-25]	[12.5-25]	[25-50]	[25-50]	[25-50]
				MBC	100	>100	>100	>100	>100	>100
4	OH	CNO_2	NH_2	MIC	[12.5-25]	[12.5-25]	[25-50]	[50-100]	[25-50]	[50-100]
				MBC	>100	>100	>100	>100	>100	>100
5	OCH_3	CH	NH_2	MIC	[6.25-12.5]	[25-50]	[25-50]	[25-50]	[25-50]	[25-50]
				MBC	>100	>100	>100	>100	>100	>100
6	OCH_3	N	NH_2	MIC	[3.13-6.25]	[25-50]	[25-50]	[25-50]	[25-50]	[25-50]
				MBC	>100	>100	>100	>100	>100	>100
7	CH_3	CH	NO_2	MIC	[6.25-12.5]	[25-50]	[12.5-25]	[12.5-25]	[25-50]	[25-50]
				MBC	>100	>100	>100	>100	>100	>100
8	OCH_3	CNO_2	NH_2	MIC	[6.25-12.5]	[25-50]	[12.5-25]	[12.5-25]	[25-50]	[25-50]
				MBC	>100	>100	>100	>100	>100	>100
9	CH_3	N	NH_2	MIC	[12.5-25]	[25-50]	[12.5-25]	[25-50]	[50-100]	[50-100]
				MBC	>100	>100	>100	>100	>100	>100
10	CH_3	CH	NH_2	MIC	[12.5-25]	[25-50]	[12.5-25]	[25-50]	[50-100]	[50-100]
				MBC	>100	>100	>100	>100	>100	>100
11	OCH_3	CH	NO_2	MIC	[6.25-12.5]	[25-50]	[12.5-25]	[25-50]	[50-100]	[50-100]
				MBC	>100	>100	100	>100	>100	>100
12	CH_3	CNO_2	NH_2	MIC	[6.25-12.5]	[12.5-25]	[12.5-25]	[25-50]	[12.5-25]	[50-100]
				MBC	>100	>100	100	>100	50	100
13	NO_2	CH	NH_2	MIC	[6.25-12.5]	[12.5-25]	[25-50]	[12.5-25]	[25-50]	[25-50]
				MBC	>100	>100	100	>100	50	100
14	NO_2	CH	NO_2	MIC	[6.25-12.5]	[12.5-25]	[25-50]	[25-50]	[12.5-25]	[25-50]
				MBC	>100	>100	>100	>100	>100	>100
15	NO_2	CNO_2	NH_2	MIC	[6.25-12.5]	[12.5-25]	[25-50]	[25-50]	[25-50]	[25-50]
				MBC	>100	>100	>100	>100	>100	>100
16	NH_2	CH	NH_2	MIC	[12.5-25]	[12.5-25]	[12.5-25]	[25-50]	[25-50]	[25-50]
				MBC	100	>100	>100	100	100	100
Levofloxacin	MIC	<1.52	<1.52	<1.52	<1.52	<1.52	<1.52			
	MBC	<1.52	<1.52	<1.52	<1.52	<1.52	<1.52			
Fusidic acid	MIC	[12.5-25]	[12.5-25]	[12.5-25]	[12.5-25]	[12.5-25]	[12.5-25]			
	MBC	100	100	>100	>100	>100	>100			

[a] [c] Concentration values are expressed in µg/mL.

Hence, against *M. luteus* the same MICs as FA were estimated for compounds **2-4, 9, 10** and **16**, and the majority of benzothiazoles (**5, 7, 8, 11-15**) showed MICs below that of FA, ranging between 6.25-12.5 μg/mL except for **6** (3.13-6.25 μg/mL). Against *S. aureus* **1** showed the strongest potency with MIC between 6.25-12.5 μg/mL, while half of the compounds (**2-4, 12-16**) exhibited the same MIC as FA (12.5-25 μg/mL). Against *E. coli, P. aeruginosa* and *S. enterica*, compounds **2, 7, 8**, and **12** displayed the higher potency with MICs similar to FA in two bacteria indistinctly, while **1** showed the same MIC as FA for the three Gram-negative strains. Only **12** and **13** displayed MBCs of 50 μg/mL for *S. enterica*. The antifungal MICs for the 2-arylbenzothiazole **1** and its 2-pyridinyl analogous **2** were comparable with FA (12.5-25 μg/mL). The rest of the benzothiazoles displayed higher inhibitory concentrations against the opportunistic pathogenic yeast *C. albicans* ranging from 25-100 μg/mL.

These results suggest that the concurrent functionalization of a hydroxyl group and an amino group as substituents in R and Y positions, respectively, has a positive influence on the antibacterial activity against Gram-positive pathogens (compound **1**) and on the antifungal activity (compounds **1** and **2**). When the hydroxyl function of compound **1** is replaced by a methoxy (compound **5**) or a nitro function (compound **13**), no difference in activity was observed against *M. luteus* (MIC values between 6.25-12.5). However, the antimicrobial activity decreases for most pathogens. The introduction of an amino group (compound **16**) has no positive influence on the activity. Therefore, a hydroxyl group may be required to exhibit notable antimicrobial effects.

3.1.2. Antibiofilm activity

The biocidal effects of the BTs were evaluated through their ability to inhibit the biofilm formation in *S. aureus* and *P. aeruginosa*. The early biofilm adherence was studied according to the minimum inhibitory concentration corresponding to each compound. All compounds exhibited antibiofilm effects in both strains. The inhibition percentages were greater than 20% for *P. aeruginosa* and above 50% for *S. aureus*, as shown in Figure 2 a) and b), respectively.

The 16 functionalized benzothiazoles exhibited good biocidal effects against Gram-negative *P. aeruginosa*, showing inhibition percentages at their MIC greater 76%. Compounds **5, 7**, and **12** with 85% of anti-adhesive activity and benzothiazole **9** (87%) showed the most prominent anti-biofilm activity on *P. aeruginosa*, significantly higher ($p < 0.001$) than both positive controls (Lv and FA) used. Unexpectedly,

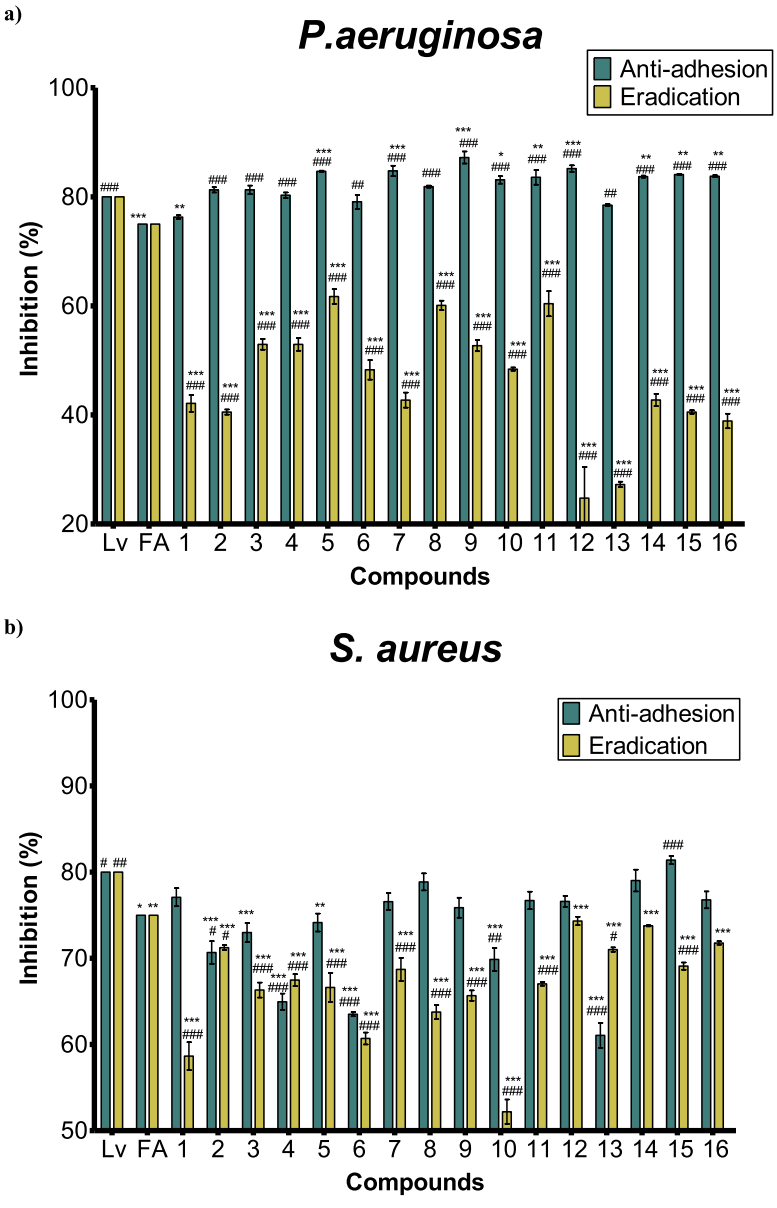

Figure 2. Inhibition percentage of the antibiofilm activity against a) *P. aeruginosa* b) *S. aureus* of levofloxacin (Lv), fusidic acid (FA), and benzothiazoles (**1-16**). Bars represent the effect at MICs (anti-adhesive)-green or at 200 μg/mL (eradication)-yellow of each BT. The percentage is the OD measured at 570 nm of treated bacteria relative to the negative control (untreated). Means ± SD for at least three independent experiments (n = 3) are shown. The levels of significance were determined using one-way ANOVA followed by Dunnett's post-test when compared to Lv: $^{***}p < 0.001$, $^{**}p < 0.01$ and $^{*}p < 0.05$, or to FA $^{###}p < 0.001$, $^{##}p < 0.01$ and $^{#}p < 0.05$ in the anti-adhesion or eradication tests, indistinctly.

most of the compounds exhibited eradication percentages of *P. aeruginosa* lower than those obtained for *S. aureus*, displaying **5** the greater value recorded of 62%.

Meanwhile, against *S. aureus*, the studied benzothiazoles **1, 7-9, 11, 12, 14, 16** displayed inhibition percentages equivalent to FA at their MIC in the anti-adhesion test as shown in Figure 2 a). In the same, compounds **14** (79%) and **15** (81%) exhibited a biocidal effect similar to levofloxacin (80%) against *S. aureus*, significantly greater than FA. In the eradication test, the antibiofilm effect of compound **12** (74%) against *S. aureus* was the most important of the set, being less than Lv but not significantly different from FA (75%).

The biocidal activity of **12** over *S. aureus* was confirmed by fluorescence microscopy (Figure 3). The images of the acridine orange staining treated slides with compound **12** confirmed the ability of this benzothiazole to alter the surface characteristics of bacterial cells and at both anti-adhesive (b) and eradication (c) concentrations when compared to untreated bacteria (a).

3.1.3. Cell viability evaluation

Effects on AhR-HepG2 proliferation caused by the studied 2-aryl and 2-pyridinylbenzothiazoles were determined *in vitro* by the MTT bioassay. The obtained cell viability expressed as a percentage of non-treated cells is represented in Figure 4.

The treatment up to 10 μM of exposure concentration with all the compounds allowed the maintenance of cell proliferation above 85%. Therefore, none of the 16 BTs evaluated was considered cytotoxic on the AhR-HepG2 cell line.

3.1.4. AhR reporter assays

The modulation of AhR-mediated expression caused by the set of BTs was evaluated in a cell-based method using AhR-HepG2 cells. In a previous study, we have reported a preliminary *in silico/in vitro* screening of the AhR agonism of diverse compounds, including some of the studied benzothiazoles herein analyzed (Goya-Jorge et al., 2020). The prominent activity exhibited by these derivatives motivated to elucidate further on the AhR effects caused by BT class of compounds as presented herein. Thus, agonistic and antagonistic bioassays were conducted *in vitro* for a greater number of benzothiazole derivatives, aiming to analyze the substituents' influence in AhR-mediated activity.

AhR antagonism. The EC_{50} of the agonist compound FICZ was 9.06 μM in this cell line, as we previously reported (Goya-Jorge et al., 2020). The antagonist bioassays were developed by co-exposure the EC_{50} of FICZ with each tested BT or else, with the known AhR antagonist CH223191. The dose-response curve obtained for CH223191 is presented in Figure 5.

The dose-response curve obtained for the control CH223191 to validate the competitive antagonist test was consistent with some other results reported in the literature (Mohammadi-Bardbori et al., 2019). However, none of the 16 benzothiazoles assayed exhibited any

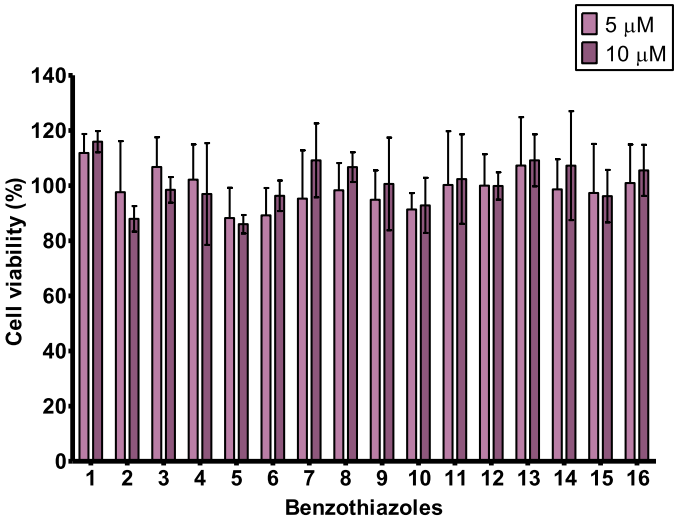

Figure 4. Viability percentages of cells exposed to the BTs by MTT assay. Compounds **1-16** were assayed at 5 μM and 10 μM. Bars represent the mean percentage ± SD from at least four independent experiments (n = 4). Compounds that reduce cell viability below 85% were considered cytotoxic. No significant differences were observed from vehicle control using one-way ANOVA followed by Dunnett's post-test ($p < 0.05$).

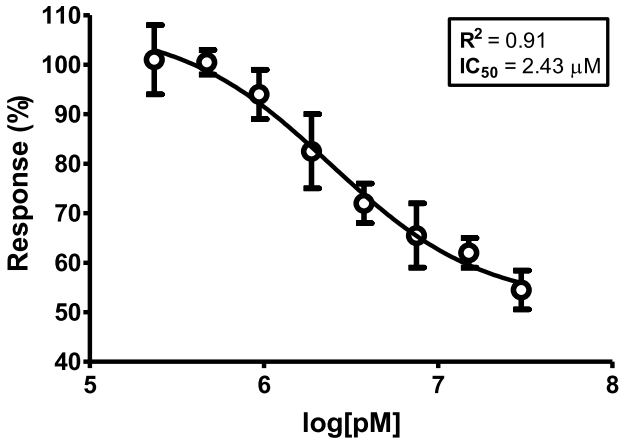

Figure 5. Dose-response curve of compound CH223191 used as positive control in the AhR antagonist assay. The dosage is represented as the logarithm of the concentration expressed in pM (1.0×10^{-12} M), while the effect is expressed as % of FICZ [EC_{50}] ± SEM. The R^2 and the IC_{50} (μM) estimated from the curve are informed.

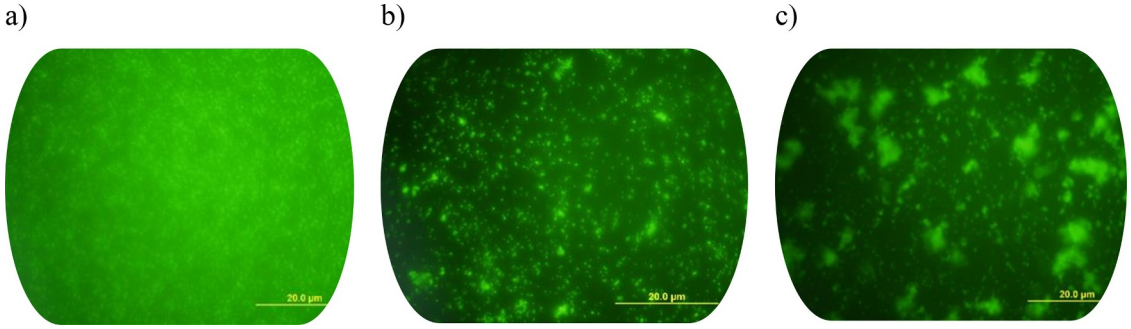

Figure 3. Fluorescence microscopy images (9× 40) of *S.aureus* biofilm formation. Green areas represent the formed biofilm and black areas indicate necrotic zones. a) Non-treated biofilm, b) Biofilm treated with compound **12** at 50 μg/mL (MIC) *i.e.* anti-adhesion activity, c) Biofilm treated with compound **12** at 200 μg/mL *i.e.* eradication activity.

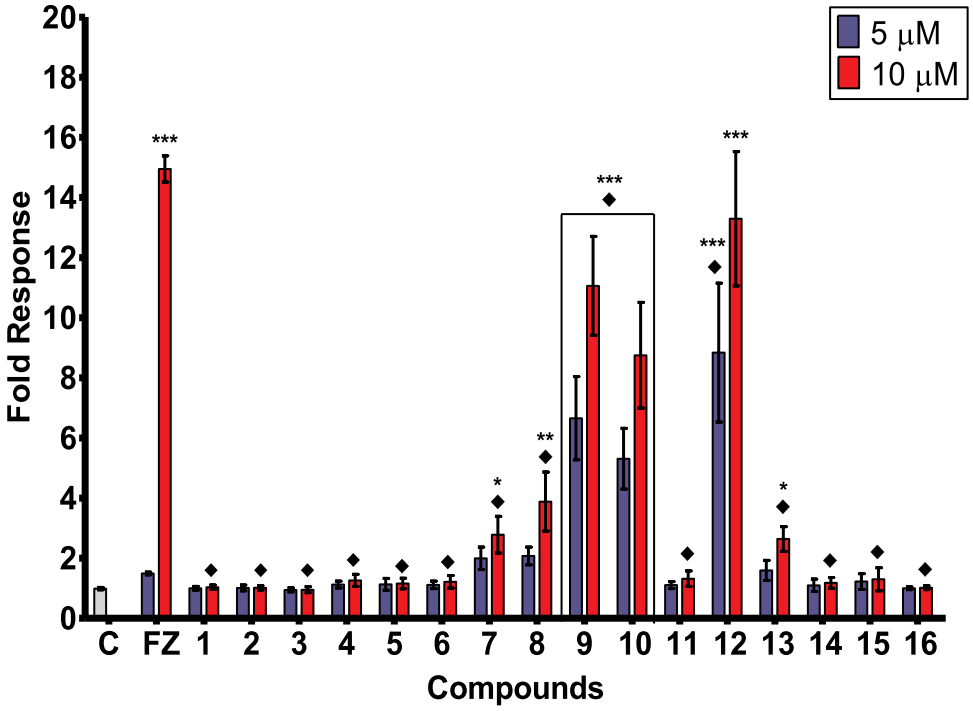

Figure 6. AhR agonistic activity (fold response) induced in AhR-HepG2 cells by the set of BTs (**1**-**16**). Bars represent means ± SD from at least four individual experiments (n = 4). The levels of significance were determined using one-way ANOVA followed by Dunnett's post-test when compared to vehicle control (**C**): ***p < 0.001, **p < 0.01 and *p < 0.05, and when compared with FICZ's effect ♦p< 0.001 at the same exposure concentration.

blockage capacity of AhR transcriptional activity, by the contrary, most of them displayed potential synergism when co-exposure with FICZ.

AhR agonism. Results obtained in the AhR agonist bioassay are represented in Figure 6 for the two assayed concentrations of the benzothiazoles, for the positive control FICZ (FZ) and for the vehicle control (C) of non-treated cells.

Overall, the set of BT derivatives exhibited a remarkable induction of AhR-mediated expression as displayed in Figure 6. Compounds **9, 10**, and **12** at both concentrations tested exhibited a very significant AhR agonist activity ($p < 0.001$) compared with the vehicle, while the positive control FICZ induced a significant activity only at the highest dosage. Moreover, compounds **7, 8**, and **13** showed a notable response when compared with non-treated cells.

The induction of AhR transcriptional activity of benzothiazole **12** at 10 μM was comparable with that displayed by the agonist FICZ, while the rest of the tested compounds exhibited effects significantly lower.

3.2. SAR considerations: antibiofilm activity vs. AhR agonism

The structural differences across the set of BTs and their influence on the antibiofilm activity and the AhR agonism were analyzed and summarized in Table 2.

As observed in Table 2, the AhR agonism was represented as a percentage of the activity displayed by FICZ (agonist efficiency). All benzothiazoles at 5 μM reached percentages higher than 50% of agonist efficiency. Compounds **7, 8**, and **13** exhibited a similar induction (~100%) of AhR transcriptional activity than the positive control at 5 μM, while **9, 10**, and **12** displayed AhR agonist efficiencies more than three times stronger than FICZ. At 10 μM, which is slightly above the EC_{50} determined for FICZ (9.06 μM), only the benzothiazole **12** induced an effect comparable (89%) with the positive control followed by compounds **9** (74%) > **10** (66%) > **8** (22%) > **13** (21%). The rest of BTs induced below 20% of FICZ's response at the highest exposure concentration. In the anti-adhesion tests where the MIC of each compound was assayed against *S. aureus* and *P. aeruginosa*, the greatest inhibition percentages in the biofilm formation for *P. aeruginosa* were identified for **9** (87%) followed by **12** = **7** = **5** (85%). Compounds **12** (74%) and **14** (73%) showed the strongest eradication of *S. aureus* followed by **16** (72%) > **13** = **2** (71%). Therefore, based on the effects displayed in both antibacterial and AhR agonist effects the following structure-activity considerations stand out:

1 AhR agonism does not seem to be determined by belonging to the 2-aryl or to the 2-pyridinylbenzothiazole subsets, noticeable when compared **1** *vs.* **2** or **5** *vs.* **6**, all of them below 10% of efficiency at 10 μM, and also when compared the strong inducers of AhR agonistic activity **9** *vs.* **10** whose efficiencies were no significantly different. Moreover, the stronger inducer of AhR-mediated effects was the arylbenzothiazole **12** followed by the pyridinylbenzothiazole **9**. Similarly, the biofilm formation of *S. aureus* and *P. aeruginosa* was not crucially determined by the aminophenyl or the aminopyridine substituent in position 2 of the benzothiazole, however, the aminopyridinyl derivative **6** exhibited lower inhibitory percentages in both anti-adherence and eradication tests when compared with its phenyl analogous **5**.
2 The *p,m*-disubstitutions with amino and nitro groups of 2-phenyl benzothiazoles, positively contributed to the AhR agonism and to the biocidal activity when compared **12** *vs.* **10**. In **8** the disubstitution significantly contributed to the AhR agonism compared to **5,** but non important differences were observed regarding the anti-adhesive or eradication effects. Lastly, the *p,m*-disubstitution positively contributed to the antibiofilm activity of **15** when compared with **13**, contrary to the AhR agonism, which was much higher in the monosubstituted **13** than in **15**.
3 The occurrence of AhR-mediated transcription was significantly higher for methyl substituents in the benzothiazole skeleton compared with all the corresponding analogous hydroxy, methoxy, nitro and amino for both 2-phenyl and 2-pyridinyl subseries (**10** *vs.* **1, 5, 13, 16**; **12** *vs.* **4, 8, 15**; **9** *vs.* **2, 6**; **7** *vs.* **3, 11, 14**).

3.3. Computational studies

3.3.1. ADMET and druglikeness profile

Benzothiazole **12** was selected by its attractive antimicrobial and AhR agonist activities to predict *in silico* its ADMET and druglikeness profile. Physicochemical and pharmacokinetic properties, as well as potential metabolic reactions predicted for **12**, are presented in Table 3.

As reported in Table 3, **12** showed acceptable physicochemical

Table 2
Summary of the AhR agonist efficiency and the biocidal activity exhibited by the sixteen benzothiazole derivatives.

BT	STRUCTURE	AhR agonist activity	Antibiofilm activity a. *S. aureus* b. *P. aeruginosa*	
		% Efficiency	% Anti-adhesion	% Eradication
01	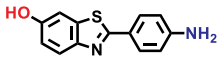	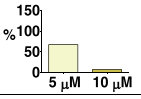	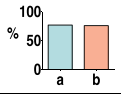	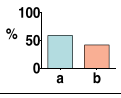
02	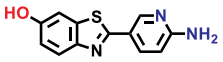	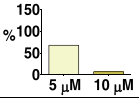	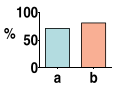	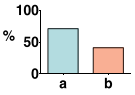
03	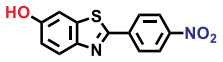	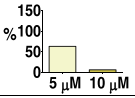	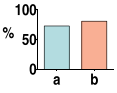	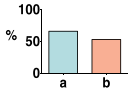
04	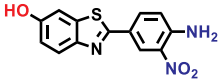	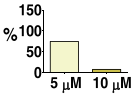	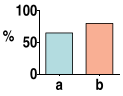	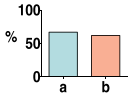
05	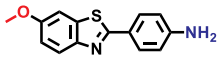	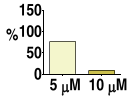	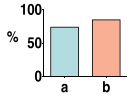	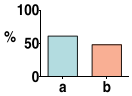
06	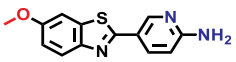	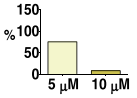	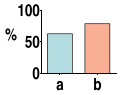	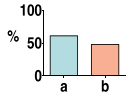
07	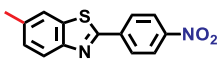	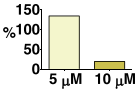	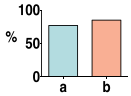	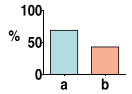
08	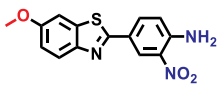	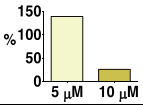	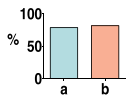	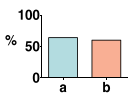
09	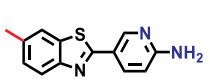	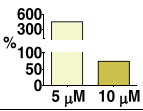	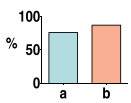	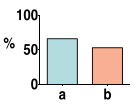
10	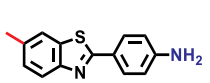	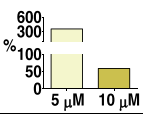	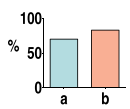	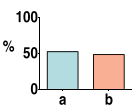
11				

parameters with not excessive lipophilicity (log P = 4.23), low solubility (Sw), dissociation (pKa) and diffusion in water (DiffC) standards as well as a not overly large structure as demonstrated by the molal volume (MolVol) of 266 cm^3/mol. High passive permeability (predicted Madin-Darby Canine Kidney (MDCK) model) and jejunal permeability (Peff) were predicted for **12**. The skin and cornea permeabilities were normal while the blood-brain barrier (BBB) penetration was identified as high.

In addition, Lipinski's rule of 5 revealed that **12** complied with molecular weight < 500, partition coefficient (logP) < 5, hydrogen bond donor ≤ 5, and hydrogen bond acceptors ≤ 10, suggesting favorable oral bioavailability for this arylbenzothiazole (data no shown).

Concerning the pharmacokinetic properties, only 1.06% was predicted as unlikely to be bond to blood plasma proteins in human (hum_fup%) with a blood to plasma ratio (RBP) of 0.12. The Volume of distribution (Vd) at steady state in humans was estimated as adequate and the Extended Clearance Classification System (ECCS) assessed a Class 2 to **12**. Such classification places metabolism as a primary clearance mechanism which is very common for drug-like compounds (Varma et al., 2015). The clearance parameters (CL_Metb, CL_Renal, CL_Uptake) corroborated the critical role of metabolism and the non-relevant contributions of the renal elimination nor the hepatic uptake for the studied molecule.

Compound **12** was predicted to be a substrate for several Phase I metabolizing enzymes of cytochrome P450 (CYP). The metabolic rate constants K_m and V_{max} were above 23 μM and below 8 nmol/min/nmol

Table 3
ADME-related physicochemical parameters, pharmacokinetic properties, and metabolic reactions predicted for benzothiazole **12**.

PHYSICOCHEMICAL										
logP[a]	pKa[b]	Sw[c]	DiffC[d]	MolVol[e]	MDCK[f]	Peff[g]	Skin[h]	Cornea[i]	BBB[j]	logBB[k]
4.23	3.73	4.79	8.29	266	5.45	4.90	1.25	1.48	High	0.15
PHARMACOKINETIC										
Hum_fup[l]	RBP[m]	V_d[n]	ECCS[o]	CL_Metb[p]	CL_Renal[q]	CL_Uptake[r]				
1.06%	0.12	0.31	Class 2	Yes (99%)	No (95%)	No (99%)				
METABOLISM										
Phase 1. Oxidation[s]	**CYP1A2**	**CYP2A6**	**CYP2B6**	**CYP2C8**	**CYP2C9**	**CYP2C19**	**CYP2D6**	**CYP2E1**	**CYP3A4**	
Substrate[t]	Yes	Yes	Yes	Yes	No	No	Yes	No	Yes	
Confidence[u]	88%	60%	55%	79%	81%	98%	82%	97%	83%	
Km[v]	23.02	-	-	-	-	-	63.02	-	55.73	
Vmax[w]	7.10	-	-	-	-	-	3.48	-	0.41	
CLint[x]	16.04	-	-	-	-	-	0.44	-	0.82	
Phase 2. Glucuronidation[y]	**UGT1A1**	**UGT1A3**	**UGT1A4**	**UGT1A6**	**UGT1A8**	**UGT1A9**	**UGT1A10**	**UGT2B7**	**UGT2B15**	
Substrate[t]	Yes	No	No	No	Yes	Yes	No	No	No	
Confidence[u]	90%	51%	72%	75%	87%	88%	86%	56%	98%	

[a] logP: octanol-water partition coefficient (lipophilicity)
[b] pKa: dissociation constant using submodels to predict protic ionization microconstants for all identified ionizable groups in a molecule.
[c] Sw (mg/mL $\times 10^{-4}$): native water solubility.
[d] DiffC ($cm^2/s \times 10^6$): molecular diffusion coefficient in water
[e] MolVol (cm^3/mol): molal volume at the normal boiling point
[f] MDCK ($cm^2/s \times 10^5$): apparent MDCK COS permeability
[g] Peff ($cm^2/s \times 10^4$): human effective jejunal permeability
[h] Skin ($cm^2/s \times 10^5$): permeability through human skin
[i] Cornea ($cm^2/s \times 10^5$): permeability through rabbit cornea
[j] BBB: qualitative likelihood (High/Low) of crossing the blood-brain barrier (98% confidence)
[k] logBB: logarithm of the brain/blood partition coefficient.
[l] Hum_fup: percent unbound to blood plasma proteins in human.
[m] RBP: blood-to-plasma concentration ratio in human.
[n] V_d (L/kg): volume of distribution in humans at steady state.
[o] ECCS Class: Extended Clearance Classification System (ECCS) assignment
[p] CL_Metab: predicts whether or not metabolism will be critical to clearance
[q] CL_Renal: predicts whether or not renal elimination will be critical to clearance.
[r] CL_Uptake: predicts whether or not hepatic uptake will be critical to clearance.
[s] Most common chemical reaction of Phase 1 of metabolism (oxidation) by Cytochromes P450 (CYP) enzymes
[t] Substrate: substrate classification models (yes/no) for human CYPxxx or UGTxxx
[u] Confidence of predictions
[v] Km (μM): estimated Michaelis-Menten Km constant for predicted sites of metabolism by human CYPxxx
[w] Vmax: [nmol/min/nmol enzyme]: estimated Michaelis-Menten V_{max} constant for predicted sites of metabolism by CYPxxx
[x] CLint (μL/min/mg human liver microsomes (HLM) protein): estimated intrinsic clearance for predicted sites of metabolism by CYPxxx
[y] Most common chemical reaction of Phase 2 of metabolism (glucuronidation) by uridine 5′-diphospho-glucuronosyltransferase (UGT)

Table 4
Human and environmental toxicological parameters predicted for benzothiazole **12**

HUMAN TOXICITY								
MaxRTD[a]	Plipidosis[b]	**Developmental and genetic toxicity**		**Human liver adverse effects**				
		Repro_Tox[c]	Mutagenesis[d]	AlkPhos[e]	GGT[f]	LDH[g]	AST[h]	ALT[i]
3.16	Nontoxic	Nontoxic	Negative	Normal	Normal	Normal	Elevated	Elevated
96%	99%	69%	99%	65%	97%	74%	85%	86%
ECOTOXICITY								
Bioconcn[j]	Biodegradn[k]	Daphnia_LC_{50}[l]	Minnow_LC_{50}[m]	Estrogenic[m]				
68.75	No (95%)	0.11	7.53	Nontoxic (98%)				

[n] Fathead minnow (*Pimephales promelas*) toxicity
[a] MaxRTD (mg/kg/day): qualitative assessment of the Maximum Recommended Therapeutic Dose administered as an oral dose.
[b] Plipidosis: qualitative estimation of potential for causing phospholipidosis.
[c] Repro_Tox: qualitative estimation of reproductive / developmental toxicity, (confidence %).
[d] Mutagenesis: classification model for the mutagenicity of pure compounds in *S. typhimurium* strain TA102 or *E. coli* strain WP2 uvrA, (confidence%).
[e] AlkPhos: human liver adverse effect as the likelihood of causing elevation in the levels of Alkaline Phosphatase enzyme, (confidence %).
[f] GGT: human liver adverse effect as the likelihood of causing elevation in the levels of gamma-glutamyl transferase (GGT) enzyme, (confidence %).
[g] LDH: human liver adverse effect as the likelihood of causing elevation in the levels of lactate dehydrogenase (LDH) enzyme, (confidence %).
[h] AST: human liver adverse effect as the likelihood of causing elevation in the levels of serum glutamic oxaloacetic transaminase (SGOT) enzyme, (confidence %).
[i] ALT: human liver adverse effect as the likelihood of causing elevation in the levels of serum glutamic pyruvic transaminase (SGTP) enzyme, (confidence %).
[j] Bioconcn (Cfish/Cwater): bioconcentration factor - partition coefficient between fish tissues and environmental water at steady state.
[k] Biodegradn: likelihood of biodegradation in the environment expressed as relative biological oxygen demand.
[l] Daphnia_LC_{50} (mg/L): LC_{50} for *Daphnia magna* (water flea) lethal toxicity after 48 hours of exposure.
[m] Estrogenic: classification model for predicting antiestrogen activity in rats (confidence %).

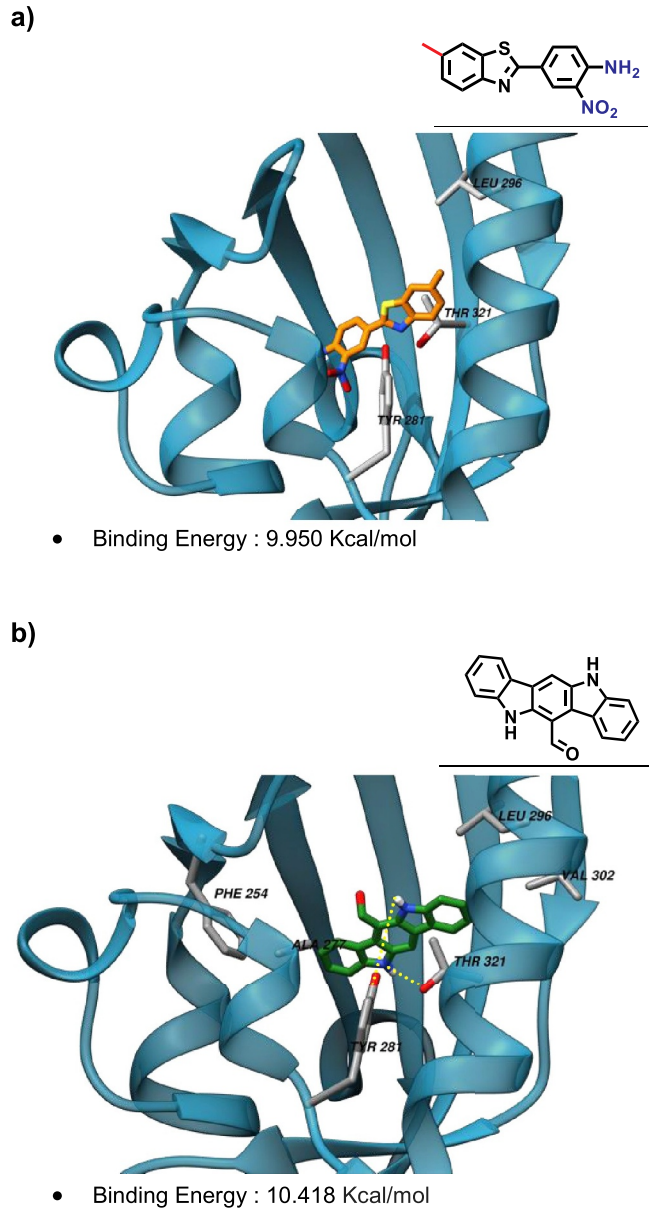

Figure 7. Molecular docking analyses for a) Benzothiazole **12** and b) **FICZ** with AhR-Ligand Binding Domain (PBD ID: 3F1O). Left side: the structure of the protein is represented as transparent blue ribbons and the best pose obtained for **12** and FICZ are displayed as sticks. The residues involved in hydrophobic interactions are labeled. Hydrogen bond interactions are represented in b) as yellow dot lines. Right side: the binding pocket residues are listed, in bold are highlight the matching between the two ligands.

enzyme, respectively. For CYP1A2, the lowest K_m and the highest V_{max} and intrinsic clearance (CLint) were predicted. Comparable K_m values were estimated for CYP2D6 and CYP3A4 (63.02 and 55.73 μM) and, while a higher V_{max} was predicted for CYP2D6 (3.48 *vs.* 0.41 nmol/min/nmol enzyme), a greater clearance was predicted for CYP3A4 (0.82 *vs.* 0.44 μL/min/mg human liver microsomes protein).

In Phase II of metabolism, **12** was predicted to be a substrate of three out of nine uridine 5′-diphospho-glucuronosyltransferase (UGT) isoforms studied. Thus, with predictive confidence above 87%, the arylbenzothiazole is probably metabolized in glucuronidation reactions mediated by UGT1A1, UGT1A8, and UGT1A9.

Finally, the global parameter ADMET_Risk was calculated in ADME Predictor software, which concisely summarizes the information from other properties and descriptors predicted to identify important liabilities in drug candidates. The risk assessment is conducted by comparing with a reference set of 2270 commercial drugs from the World Drug Index (WDI) of which 90% have an ADMET_Risk score lower than 7. For **12**, a score of 3.75 was predicted as ADMET_Risk.

Toxicological indexes for humans and for ecosystems were also predicted for **12** (Table 4). Hence, the arylbenzothiazole was not predicted as a potential trigger of phospholipidosis nor as a reproductive or mutagenic agent. Regarding the hepatotoxicity, elevated levels of the two transaminases (AST and ALT) and normal levels of the rest of the enzymes were predicted. Therefore, **12** was not predicted to cause relevant harm to humans. Meanwhile, the ecotoxicological parameters *in silico* estimated for **12**, standing out the prediction of a poor biodegradability and an unlike probability of causing endocrine disruption via the estrogen receptor.

3.3.2. Molecular docking analysis

The binding interactions with the ligand binding domain of AhR were explored through molecular docking for **12** and for the known agonist FICZ and the outcome is presented in Figure 7 a) and b), respectively.

The binding energy with AhR, as well as the pocket residues identified in the molecular docking simulations, were similar for the arylbenzothiazole and for the ligand/agonist FICZ as represented in Figure 7. Furthermore, the THR 321 residue was predicted to interact hydrophobically with **12** and FICZ, while TYR 281 and LEU 296 seemed to establish hydrophobic interactions with **12** and hydrogen bonds with FICZ.

4. Conclusions

Ah receptor is an important chemical sensor that integrates dietary, environmental, metabolic, and microbial signals to regulate transcriptional programs in a context, cell type, and ligand-specific manner. The association of AhR with the immune system has been widely studied, particularly important in gut microbiota and barrier tissues, where crucial immune responses are related to AhR expression. The dual association of antimicrobial and AhR modulatory effects could be potentially beneficial in drug discovery. Hence, in this work, both effects were evaluated for a set of functionalized benzothiazoles yielding a promising activity for one derivative **12** as biocidal against *S. aureus* and as AhR agonist. Structure-activity analyses revealed general headlines on the substituent's contributions. Finally, computational studies with benzothiazole **12** predicted an adequate ADMET profile and a potentially similar binding to AhR when compared with the known agonist FICZ.

Abreviation

ADMET	absorption, distribution, metabolism, and excretion - toxicity
AhR	aryl hydrocarbon receptor
AhR-HepG2, Lucia™	human hepatoma cell line stably transfected to express AhR
BT	benzothiazole
CH223191	2-methyl-2H-pyrazole-3-carboxylic acid
CYP	cytochrome P450
Eff	efficiency
FA	fusidic acid
FICZ	5,11-dihydroindolo[3,2-b]carbazole-12-carbaldehyde
Lv	levofloxacin
MBC	Minimal Bactericidal Concentration
MIC	Minimal Inhibitory Concentration
MTT	3-(4,5-dimethyl thiazol-2-yl)-2,5-diphenyl tetrazolium bromide
OD	optical density

Author Contributions

All authors contributed to the drafting and revision of the article and approved the final version.

Credit Author Statement

E.G.J accomplished biological experiments to evaluated AhR expression ability, data curation, and structure-activity relationship analyses. F. A performed antibacterial, antifungal, and biocidal evaluation. L.E.C accomplished molecular docking studies. R. M. G designed and supervised biological studies. M.S-IV was responsible for chemicals supply, structure-activity and biological analysis and supervised the project. All authors contributed to the drafting and revision of the article and approved the final version presented.

Declaration of Competing Interest

The authors declare no conflict of interest.

Acknowledgments

We gratefully acknowledged the “PHC Utique” programme of the French Ministry of Foreign Affairs and Ministry of higher education, research and innovation and the Tunisian Ministry of higher education and scientific research in the CMCU project number 17G1215 for financial support of this work. This project has received funding from the European Union's Horizon 2020 research and innovation programme under the Marie Skłodowska-Curie grant agreement No. 722634. FA thanks to Mouna Jlidi for assisting her during the antibiofilm activity evaluation.

References

Ali, R., Siddiqui, N., 2013. Biological aspects of emerging benzothiazoles: A short review. J. Chem 2013. https://doi.org/10.1155/2013/345198.

Bessede, A., Gargaro, M., Pallotta, M.T., Matino, D., Servillo, G., Brunacci, C., Bicciato, S., Mazza, E.M.C., Macchiarulo, A., Vacca, C., Iannitti, R., Tissi, L., Volpi, C., Belladonna, M.L., Orabona, C., Bianchi, R., Lanz, T.V., Platten, M., Della Fazia, M.A., Piobbico, D., Zelante, T., Funakoshi, H., Nakamura, T., Gilot, D., Denison, M.S., Guillemin, G.J., Duhadaway, J.B., Prendergast, G.C., Metz, R., Geffard, M., Boon, L., Pirro, M., Iorio, A., Veyret, B., Romani, L., Grohmann, U., Fallarino, F., Puccetti, P., 2014. Aryl hydrocarbon receptor control of a disease tolerance defence pathway. Nature 511, 184–190. https://doi.org/10.1038/nature13323.

Bondock, S., Fadaly, W., Metwally, M.A., 2010. Synthesis and antimicrobial activity of some new thiazole, thiophene and pyrazole derivatives containing benzothiazole moiety. Eur. J. Med. Chem. 45, 3692–3701. https://doi.org/10.1016/j.ejmech.2010.05.018.

Bort, G., Sylla-Iyarreta Veitía, M., Ferroud, C, 2013. Straightforward synthesis of PET tracer precursors used for the early diagnosis of Alzheimers disease through Suzuki-Miyaura cross-coupling reactions. Tetrahedron 69, 7345–7353. https://doi.org/10.1016/j.tet.2013.06.085.

Choudhary, S., Jeyabalan, G., Kalra, N., 2017. A Review: Therapeutic and Biological Activity of Benzothiazole Derivatives. Int. J. Recent Adv. Sci. Technol. 4, 8–20. https://doi.org/10.30750/ijrast.432.

Esser, C., Rannug, A., 2015. The aryl hydrocarbon receptor in barrier organ physiology, immunology, and toxicology. Pharmacol. Rev. 67, 259–279. https://doi.org/10.1124/pr.114.009001.

Esser, C., Rannug, A., Stockinger, B., 2009. The aryl hydrocarbon receptor in immunity. Trends Immunol 30, 447–454. https://doi.org/10.1016/j.it.2009.06.005.

Ghosh, J., Lawless, M.S., Waldman, M., Gombar, V., Fraczkiewicz, R., 2016. Modeling ADMET. In: Benfenati, E. (Ed.), Silico Methods for Predicting Drug Toxicity. Springer, New York, New York, NY, pp. 63–83. https://doi.org/10.1007/978-1-4939-3609-0_4.

Gill, R.K., Rawal, R.K., Bariwal, J., 2015. Recent advances in the chemistry and biology of benzothiazoles. Arch. Pharm. (Weinheim). 348, 155–178. https://doi.org/10.1002/ardp.201400340.

Goya-Jorge, E., Giner, R.M., Veitía, M.S.-I., Gozalbes, R., Barigye, S.J., 2020. Predictive modeling of aryl hydrocarbon receptor (AhR) agonism. Chemosphere 256, 127068. https://doi.org/10.1016/j.chemosphere.2020.127068.

Goya-Jorge, E., Rampal, C., Loones, N., Barigye, S.J., Carpio, L.E., Gozalbes, R., Ferroud, C., Veitía, M.S.-I., Giner, R.M., 2020. Targeting the Aryl Hydrocarbon Receptor with a novel set of Triarylmethanes. Eur. J. Med. Chem Submitted for publication.

Hergesheimer, R., Lanznaster, D., Vourc'h, P., Andres, C., Bakkouche, S., Beltran, S., Blasco, H., Corcia, P., Couratier, P., 2015. Advances in pharmacotherapy for the treatment of gout. Expert Opin. Pharmacother. 6566, 1–8. https://doi.org/10.1517/14656566.2015.997213.

Hu, W., Sorrentino, C., Denison, M.S., Kolaja, K., Fielden, M.R., 2007. Induction of Cyp1a1 is a nonspecific biomarker of aryl hydrocarbon receptor activation: Results of large scale screening of pharmaceuticals and toxicants in vivo and in vitro. Mol. Pharmacol. 71, 1475–1486. https://doi.org/10.1124/mol.106.032748.

Janeway, C., Travers, P., Walport, M., 2001. Manipulating the immune response to fight infection, in: Immunobiology: The Immune System in Health and Disease. Garland Science, New York.

Kamal, A., Syed, M.A.H., Mohammed, S.M., 2015. Therapeutic potential of benzothiazoles: A patent review (2010-2014). Expert Opin. Ther. Pat. 25, 335–349. https://doi.org/10.1517/13543776.2014.999764.

Keam, S.J., Croom, K.F., Keating, G.M., 2005. Levofloxacin. A review of its use in the treatment of bacterial infections in the United States. Drugs 63, 2769–2802. https://doi.org/10.2165/00003495-200565050-00007.

Krieger, E., Vriend, G., 2014. YASARA View - molecular graphics for all devices - from smartphones to workstations. Bioinformatics 30, 2981–2982. https://doi.org/10.1093/bioinformatics/btu426.

Mathis, C.A., Wang, Y., Holt, D.P., Huang, G.F., Debnath, M.L., Klunk, W.E., 2003. Synthesis and evaluation of 11C-labeled 6-substituted 2-arylbenzothiazoles as amyloid imaging agents. J. Med. Chem. 46, 2740–2754. https://doi.org/10.1021/jm030026b.

Mohammadi-Bardbori, A., Omidi, M., Arabnezhad, M.R., 2019. Impact of CH223191-Induced Mitochondrial Dysfunction on Its Aryl Hydrocarbon Receptor Agonistic and Antagonistic Activities. Chem. Res. Toxicol. 32, 691–697. https://doi.org/10.1021/acs.chemrestox.8b00371.

Mosmann, T., 1983. Rapid colorimetric assay for cellular growth and survival: Application to proliferation and cytotoxicity assays. J. Immunol. Methods 65, 55–63. https://doi.org/10.1016/0022-1759(83)90303-4.

Moura-Alves, P., Faé, K., Houthuys, E., Dorhoi, A., Kreuchwig, A., Furkert, J., Barison, N., Diehl, A., Munder, A., Constant, P., Skrahina, T., Guhlich-Bornhof, U., Klemm, M., Koehler, A.B., Bandermann, S., Goosmann, C., Mollenkopf, H.J., Hurwitz, R., Brinkmann, V., Fillatreau, S., Daffe, M., Tümmler, B., Kolbe, M., Oschkinat, H., Krause, G., Kaufmann, S.H.E., 2014. AhR sensing of bacterial pigments regulates antibacterial defence. Nature 512, 387–392. https://doi.org/10.1038/nature13684.

Moyer, J.H., Ford, R.V, 1958. Laboratory and clinical observations on ethoxzolamide (Cardrase) as a diuretic agent. Am. J. Cardiol. 1, 497–504. https://doi.org/10.1016/0002-9149(58)90121-8.

Muthusubramanian, L., Rao, V.S.S., Mitra, R.B., 2001. Efficient synthesis of 2-(thiocyanomethylthio)benzothiazole. J. Clean. Prod. 9, 65–67. https://doi.org/10.1016/S0959-6526(00)00031-7.

Oh, S., Go, G.W., Mylonakis, E., Kim, Y., 2012. The bacterial signalling molecule indole attenuates the virulence of the fungal pathogen Candida albicans. J. Appl. Microbiol. 113, 622–628. https://doi.org/10.1111/j.1365-2672.2012.05372.x.

Pettersen, E.F., Goddard, T.D., Huang, C.C., Couch, G.S., Greenblatt, D.M., Meng, E.C., Ferrin, T.E., 2004. UCSF Chimera—A visualization system for exploratory research and analysis. J. Comput. Chem. 25, 1605–1612. https://doi.org/10.1002/jcc.20084.

Ricco, C., Abdmouleh, F., Riccobono, C., Guenineche, L., Martin, F., Goya-Jorge, E., Lagarde, N., Liagre, B., Ali, M.Ben, Ferroud, C., Arbi, M.El, Veitía, M.S.-I., 2020. Pegylated triarylmethanes: Synthesis, antimicrobial activity, anti-proliferative behavior and in silico studies. Bioorg. Chem. 96, 103591. https://doi.org/10.1016/j.bioorg.2020.103591.

Salentin, S., Schreiber, S., Haupt, V.J., Adasme, M.F., Schroeder, M., 2015. PLIP: Fully automated protein-ligand interaction profiler. Nucleic Acids Res 43, W443–W447. https://doi.org/10.1093/nar/gkv315.

Shereen, M.A., Khan, S., Kazmi, A., Bashir, N., Siddique, R., 2020. COVID-19 infection: Origin, transmission, and characteristics of human coronaviruses. J. Adv. Res. 24, 91–98. https://doi.org/10.1016/j.jare.2020.03.005.

Sommer, F., Bäckhed, F., 2013. The gut microbiota-masters of host development and physiology. Nat. Rev. Microbiol. 11, 227–238. https://doi.org/10.1038/nrmicro2974.

Trott, O., Olson, A.., 2009. Software News and Update. AutoDock Vina Improving the Speed and Accuracy of Docking with a New Scoring Function, Efficient Optimization, and Multithreading. J. Comput. Chem 31, 455–461. https://doi.org/10.1002/jcc.21334.

Varma, M.V., Steyn, S.J., Allerton, C., El-Kattan, A.F., 2015. Predicting Clearance Mechanism in Drug Discovery: Extended Clearance Classification System (ECCS). Pharm. Res. 32, 3785–3802. https://doi.org/10.1007/s11095-015-1749-4.

Zhao, H., Chen, L., Yang, T., Feng, Y.L., Vaziri, N.D., Liu, B.L., Liu, Q.Q., Guo, Y., Zhao, Y.Y., 2019. Aryl hydrocarbon receptor activation mediates kidney disease and renal cell carcinoma. J. Transl. Med. 17, 1–14. https://doi.org/10.1186/s12967-019-2054-5.